

Table of contents

Experimental section.....	3
Materials.....	3
Photodeposition.....	3
Photocatalytic experiments.....	3
Characterizations.....	5
Analysis.....	5
Gas phase analysis by GC-BID detector.....	5
Liquid phase analysis by GC-FID.....	6
Water content.....	8
NMR analysis.....	8
Turn over frequency (TOF).....	8
Blank tests.....	9
Optimisation.....	10
Titanium dioxide morphology.....	10
Metal loading for cross-coupling reactions.....	11
Selectivity: N ₂ O vs. O ₂	12
Benzylamine homo-coupling with molecular sieve.....	15
Recycling tests.....	16
NMR data.....	17
NMR spectra.....	20
References.....	22

Table of figures and tables

Figure S1: Calibration curves of nitrous oxide (in green), nitrogen (in black), oxygen (in grey), and carbon dioxide (in yellow) measured by GC-BID.....	5
Figure S2: Calibration curves of benzylamine (orange circles) and 4-methoxybenzylamine (grey triangles), obtained by GC-FID with chlorobenzene as internal standard.	6
Figure S3: Calibration curves of hexylamine (blue circles), butylamine (grey squares), heptylamine (yellow triangles) and octylamine (green diamond), obtained by GC-FID with chlorobenzene as internal standard.	7
Figure S4: Calibration curves of cyclohexanemethylamine obtained by GC-FID with chlorobenzene as internal standard.	7
Figure S5: Calibration curves of dibenzylamine (blue circles) and dihexylamine (orange triangles), obtained by GC-FID with chlorobenzene as internal standard.	7
Figure S6: Calibration curve of benzyl alcohol, obtained by GC-FID with chlorobenzene as internal standard.	8
Figure S7: Kinetics for the influence of the metal loading (a: 1 mol%, b: 0.1 mol%) on the cross-coupling of benzyl alcohol and hexylamine under N ₂ O atmosphere.	11
Figure S8: Kinetics for homo-coupling of benzylamine under N ₂ O atmosphere (a), and O ₂ atmosphere (b).	12
Figure S9: Kinetics for homo-coupling of hexylamine under N ₂ O atmosphere (a), and O ₂ atmosphere (b).	13
Figure S10: Kinetics for cross-coupling of benzyl alcohol and hexylamine under N ₂ O atmosphere (a), and O ₂ atmosphere (b).	14
Figure S11: Kinetics of benzylamine homo-coupling under anhydrous conditions in the presence of molecular sieve.....	15
Figure S12: Recycling tests of the catalyst in the photo-oxidative coupling of benzylamine.	16
Figure S13: ¹ H NMR spectra after photo-oxidation of N-methylbenzylamine under standard conditions to check methylamine formation (unpurified mixture) (400 MHz, CD ₃ CN).	17
Figure S14: ¹³ C NMR spectra after photo-oxidation of N-methylbenzylamine under standard conditions to check methylamine formation (unpurified mixture) (100 MHz, CD ₃ CN).	18
Figure S15: ¹³ C NMR spectra after photo-oxidation of N-methylbenzylamine with activated molecular sieves to check methylamine formation (unpurified mixture) (100 MHz, (CD ₃) ₂ CO).	19

Experimental section

Materials

All the organic compounds were purchased from Acros Organics (Illkirch, France), TCI Europe N.V. (France), or Sigma-Aldrich-Fluka (Saint-Quentin-Fallavier, France). Silver nitrate (AgNO_3) was purchased from Acros Organics (Illkirch, France). The titanium dioxide, either anatase or rutile allotropic forms, as well as the P25 mix were obtained from Sigma-Aldrich (Saint-Quentin-Fallavier, France). Nitrous oxide 99.99% purity was purchased from Air Liquide (Paris, France). All these starting materials were used without further purification. Water was distilled twice before use by conventional method. Organic solvents were all HPLC grade.

The LED lamps were purchased from HepatoChem (EvoluChem™ LED; wavelength: 365 nm; 18W). UV intensity, or surface power density, in mW/cm^2 unit at 365 nm was measured with a radiometer VLX-3W (Vilber) with a 365 nm sensor. The UVA lamp was a Philips high-pressure Hg lamp (reference PL-L 24W/10/4P; 350-400 nm with λ_{max} around 360 nm).

Photodeposition

In a round bottom flask, an adequate amount of TiO_2 (3-4g) was added to 80 mL of an aqueous AgNO_3 solution ($9.42 \cdot 10^{-5}$ – $1.24 \cdot 10^{-4}$ mol, depending on the amount of TiO_2 to have a metal loading of 0.3 wt%), under stirring. The pH was adjusted to approximately 6.3 by addition of a few drops of a potassium hydroxide solution ($0.1 \text{ mol} \cdot \text{L}^{-1}$). After 15 min under stirring, 4 mL of methanol were added and the suspension was irradiated by a UVA lamp (Philips) for 4 hours, under continuous argon bubbling flow and vigorous stirring. The solid product was recovered by filtration of the suspension, washed several times with re-distilled water under air atmosphere, and dried under vacuum at 100°C for 1h30. The obtained photocatalyst, slightly purplish due to formation of silver oxides,¹ was grinded manually, and stored in air and away from the light.

Photocatalytic experiments

Photocatalytic experiments were performed at room temperature under nitrous oxide atmosphere (1 bar). A 10 mL schlenk tube, closed by a septum and containing the right amount of photocatalyst, is filled with nitrous oxide (three vacuum-nitrous oxide cycles) while stirring with a cross-shape magnetic stirrer. 3 mL of a solution of the amine (1 equivalent) in acetonitrile (containing also 1 equivalent of the alcohol for the cross-coupling reactions), that has been previously bubbled and stored under nitrous oxide atmosphere, was added with a syringe. The volume of the gas phase in the vessel was 1.2 equivalent of nitrous oxide (7 mL, 0.29 mmol). After stirring for 30 min in the dark to reach adsorption equilibrium conditions, the reactor was irradiated by two LED lamps at 365 nm with an average intensity around the reactor of $160 \text{ mW}/\text{cm}^2$. Due to the light irradiation, the temperature of the media reached 38°C after 15 min and remained stable afterwards. Before and after the reaction, gas phase samples were collected with a $100 \mu\text{L}$ (*i.e.* 1% of the total volume of the vessel) Hamilton Gastight SampleLock syringe, equipped with a syringe guide, and analyzed by GC for quantification (details in the analyses part). The syringe was left open and purged three times with air between each sampling. After the reaction, the reactor was opened to air and the solution was filtered through a $0.20 \mu\text{m}$ syringe filter to remove the catalyst. The solution was then analyzed by GC for quantification with chlorobenzene as internal standard (details in the analyses part).

For homo-coupling of amines, conversion, yield and selectivity were obtained according to the following equations (n_i : initial substrate molar quantity; n_f : final substrate molar quantity; n_p : product molar quantity).

$$\text{Conversion (\%)} = \frac{n_i - n_f}{n_i} \times 100$$

$$\text{Yield (\%)} = \frac{n_p}{0.5 n_i} \times 100$$

$$\text{Selectivity (\%)} = \frac{n_p}{0.5(n_i - n_f)} \times 100$$

For cross-coupling of amines and alcohols, conversion, yield and selectivity were obtained according to the following equations (n_i : initial alcohol molar quantity; n_f : final alcohol molar quantity; n_p : product molar quantity).

$$\text{Conversion (\%)} = \frac{n_i - n_f}{n_i} \times 100$$

$$\text{Yield (\%)} = \frac{n_p}{n_i} \times 100$$

$$\text{Selectivity (\%)} = \frac{n_p}{n_i - n_f} \times 100$$

Characterizations

For characterizations data of the catalyst (ICP-OES, XRD, Specific surface measurements, UV-visible spectra and TEM pictures), see our previous work.²

Analysis

Gas phase analysis by GC-BID detector

Gas chromatography was performed using a Shimadzu apparatus (Nexis GC-2030) with a BID (Barrier Ionization Discharge) detector, equipped with a Restek ShinCarbon ST micropacked column (3 m × 0.53 mm). Parameters were as follows: isotherm temperature was maintained at 40 °C for 4 min, then increased to 80 °C with a ramp of 5 °C/min (maintained 1.5 min). Injector temperature, 150 °C; detector temperature, 280 °C; manual injection; volume, 100 μL; splitless; carrier gas (He), 490.9 kPa, 100 mL/min. The final chromatogram was recorded and treated using ChromQuest software. Products identification was performed by comparison of their retention times with commercial products. Analyses were performed at least twice to control a potential air contamination. Quantification of gaseous compounds (nitrogen, nitrous oxide, oxygen, and carbon dioxide to quantify a potential mineralization) was performed thanks to the calibration curves bellow, and thanks to the following equation.

$$n_{\text{gas}} = \frac{A \times \rho \times Vg}{a \times M \times Vi}$$

n_{gas} : molar quantity of the gaseous compound (mol)

A: peak area of the compound measured by GC

ρ : density of the compound at atmospheric pressure and 15 °C (g/mL)

Vg : volume of the reactor gas phase (mL) (equal to 7 mL in this work)

M: molar mass (g/mol)

Vi : injected volume (mL) (equal to 100 μL in this work)

a: slope of the calibration curve with $A = a.Vi$

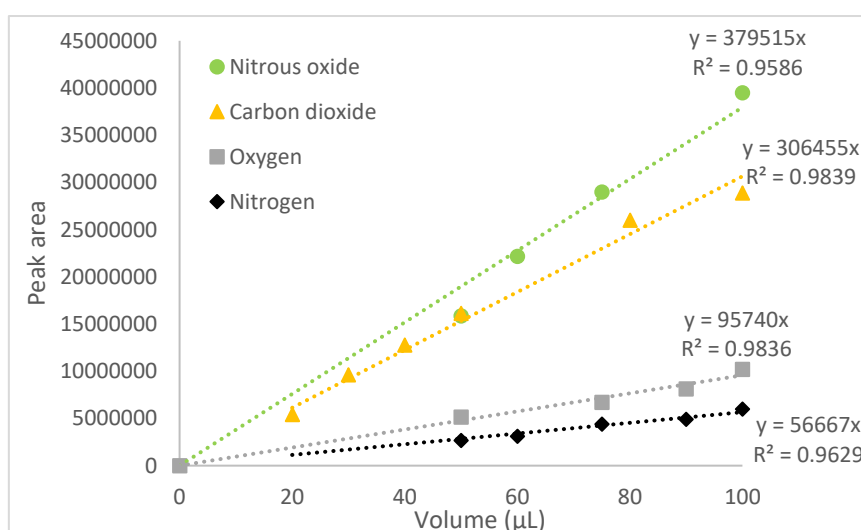


Figure S1: Calibration curves of nitrous oxide (in green), nitrogen (in black), oxygen (in grey), and carbon dioxide (in yellow) measured by GC-BID.

Liquid phase analysis by GC-FID

Gas chromatography was performed using a Shimadzu apparatus (GC-2014) with an FID detector, equipped with a SH-Rtx-5 column (30 m × 0.25 mm × 1 μm). Parameters were as follows: isotherm temperature was maintained at 50 °C for 4.93 min, then increased to 72 °C with a ramp of 5 °C/min, then increased to 80 °C with a ramp of 2 °C/min, and finally increased to 250 °C with a ramp of 30 °C/min (maintained 5 min or 25 min for heavier compounds). Injector temperature, 250 °C; detector temperature, 280 °C; injection volume, 1 μL; split flow, 1.62 mL/min; carrier gas (He), 36.9 mL/min. The final chromatogram was recorded and treated using ChromQuest software. Products identification was performed by comparison of their retention times with commercial products. Conversion and yield were determined by standard calibration with chlorobenzene as an internal standard.

Quantification analyses were achieved by an internal standard calibration procedure. Different calibration standards of the analyte were prepared. A constant amount of the standard (chlorobenzene) was added in each of the calibration standards, which were then analyzed by GC. Calibration curves were obtained by plotting the ratio of the analyte peak area to the standard peak area, versus the ratio of the analyte molar quantity to the standard molar quantity. For the quantitative analysis of experiments, a known amount of the internal standard was added into the reaction media, which was then analyzed by GC. The molar quantities in the reaction media were obtained from the equation of the calibration curves. The calibration curves below were used for quantification of the corresponding compounds.

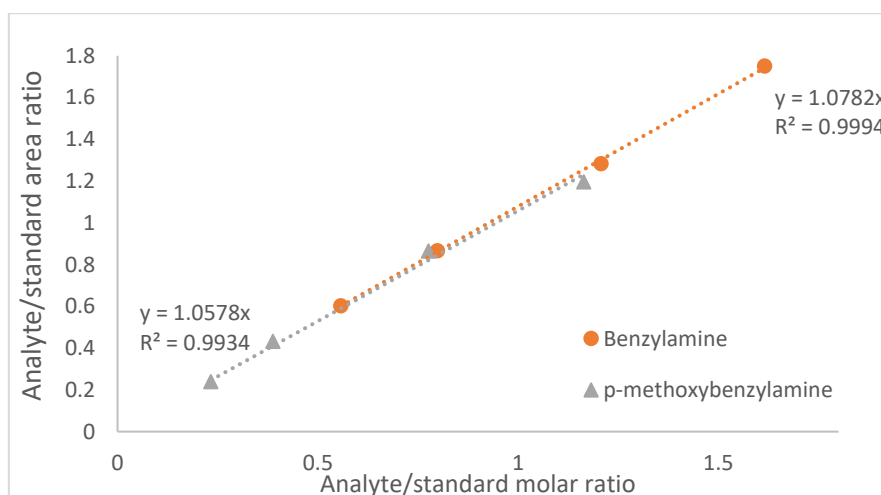


Figure S2: Calibration curves of benzylamine (orange circles) and 4-methoxybenzylamine (grey triangles), obtained by GC-FID with chlorobenzene as internal standard.

Calibration curve of 4-methoxybenzylamine was used for quantification of 2-methoxybenzylamine and 3-methoxybenzylamine.

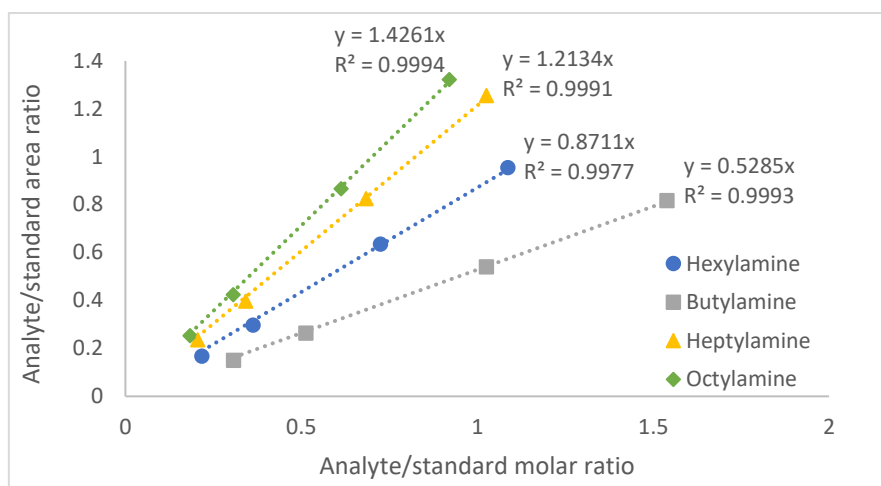


Figure S3: Calibration curves of hexylamine (blue circles), butylamine (grey squares), heptylamine (yellow triangles) and octylamine (green diamond), obtained by GC-FID with chlorobenzene as internal standard.

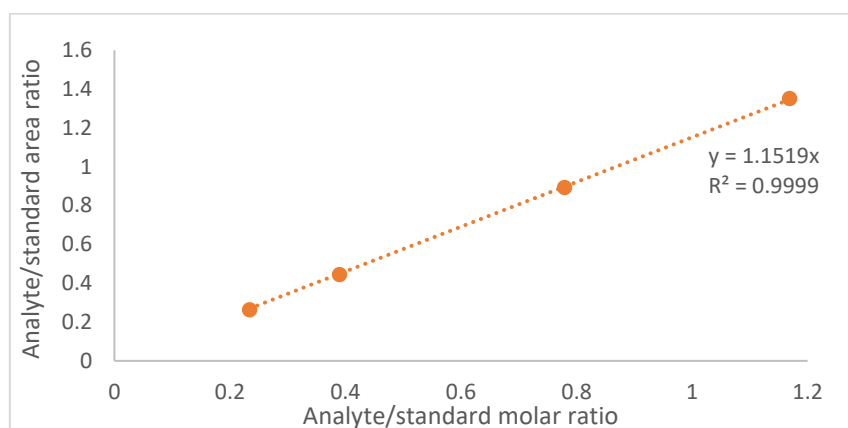


Figure S4: Calibration curves of cyclohexanemethylamine obtained by GC-FID with chlorobenzene as internal standard.

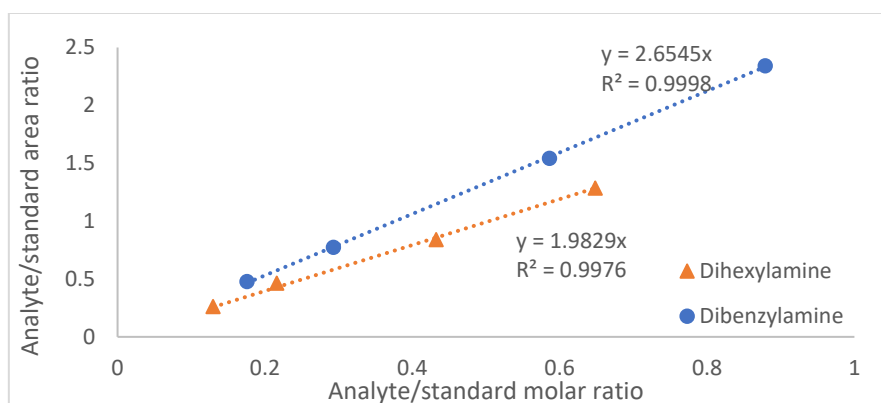


Figure S5: Calibration curves of dibenzylamine (blue circles) and dihexylamine (orange triangles), obtained by GC-FID with chlorobenzene as internal standard.

Calibration curve of dihexylamine was used for quantification of *N*-Hexyl-1-hexanimine. Calibration curve of dibenzylamine was used for quantification of *N*-benzyl-1-phenylmethanimine.

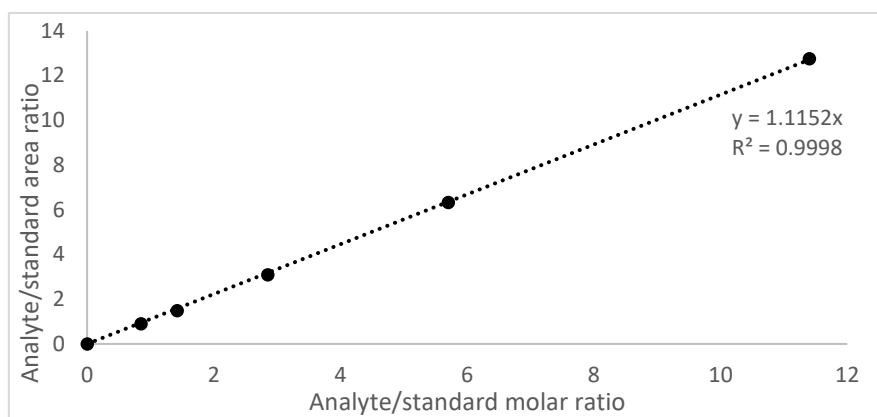


Figure S6: Calibration curve of benzyl alcohol, obtained by GC-FID with chlorobenzene as internal standard.

Calibration curve of benzyl alcohol was used for quantification of *m*-nitrobenzyl alcohol, *p*-nitrobenzyl alcohol, *o*-methoxybenzyl alcohol, *m*-methoxybenzyl alcohol and *p*-methoxybenzyl alcohol.

Water content

Evolution of water concentration during the reaction was determined with a Karl Fisher titrator equipped with a magnetic stirrer (890 Titrando, Metrohm).

NMR analysis

^1H and ^{13}C NMR spectra were recorded at room temperature on a Bruker Avance III 400 MHz spectrometer at the Ecole Nationale Supérieure de Chimie de Rennes, at 400 MHz for ^1H , and 100 MHz for ^{13}C , in CDCl_3 (residual solvent peaks: ^1H , 7.26 ppm; ^{13}C , 77.16 ppm), C_6D_6 (residual solvent peaks: ^1H , 7.16 ppm; ^{13}C , 128.06 ppm), CD_3CN (residual solvent peaks: ^1H , 2.14 ppm; ^{13}C , 118.26 ppm, 1.32 ppm), or $(\text{CD}_3)_2\text{CO}$ (residual solvent peaks: ^{13}C , 206.26 ppm, 29.84 ppm).

Turn over frequency (TOF)

Turn over frequencies were calculated according to the following equation (n_i : initial substrate molar quantity; n_f : final substrate molar quantity, MAS: metal active sites, t: time in hour), for values after a reaction time of 5 minutes (low substrate conversion) and with the true number of active sites³:

$$\text{TOF (h}^{-1}\text{)} = \frac{n_i - n_f}{\text{MAS} \times t}$$

For cross-coupling reactions, quantities of alcohol were considered.

MAS (mol): number of silver active sites, calculated according to the following equation (n : number of layers of the cluster, n_{Ag} : total silver quantity in mol, N_A : Avogadro constant, $6.02 \cdot 10^{23} \text{ mol}^{-1}$, V_g : metal atom volume, D : nanoparticle mean diameter determined by TEM):

$$\text{MAS (mol)} = (10n^2 + 2) \times n_{\text{Ag}} \times N_A \times \frac{3V_g}{4\pi(0.5D)^3}$$

With n : number of layers of the cluster, calculated according to the following equation (D : nanoparticle mean diameter determined by TEM, r : silver ray):

$$n = \left(\frac{D}{r} - 2 \right) \div 3.157$$

Blank tests

Table S1: Blank tests for photocatalytic oxidative coupling of benzylamine into N-benzyl-1-phenylmethanimine (**4**). ^a

Entry	Variation from standard conditions	Conv. (%) ^b	Yield (%) ^b	Sel. (%) ^c
1	-	>99	87	87
2	No catalyst	<1	-	-
3	No light	7	2	-
4	TiO ₂ (100 mg) instead of Ag/TiO ₂ , 2h	20	<1	-
5	TiO ₂ (100 mg) instead of Ag/TiO ₂ , O ₂ atmosphere.	>99	59	59
6 ^d	-	>99	83 ^e	-

^a Reaction conditions: benzylamine (0.24 mmol, 1 eq.), 3 mL MeCN, N₂O atmosphere (0.29 mmol in gas phase, 7 mL, 1.2 eq.), 100 mg Ag/TiO₂ (0.3 wt%, TiO₂ Aeroxide P25), *i.e.* substrate/metal = 100, 365 nm irradiation (two LEDs, 150 mW/cm²), 15 min. ^b Determined by Gas Chromatography analyses using chlorobenzene as internal standard. ^c Selectivity in imine product = yield/conversion. ^d 4 times higher scale, *i.e.* 104 μ L of starting amine instead of 26 μ L. ^e Isolated yield.

Optimisation

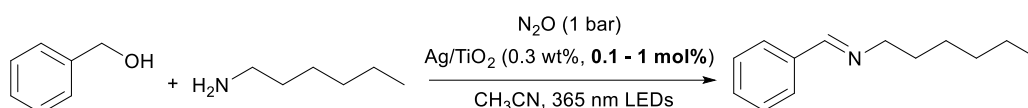
Titanium dioxide morphology

Table S2: Variation of the morphology of titanium dioxide for photooxidative coupling of benzylamine under N₂O atmosphere. ^a

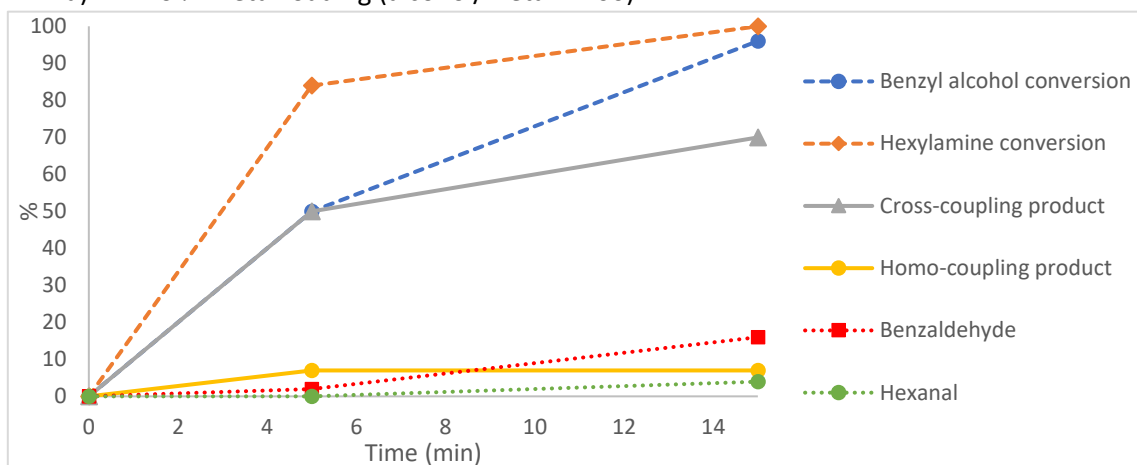
Entry	TiO ₂	Conv. (%) ^b	Yield (%) ^b	Sel. (%) ^c	TOF (h ⁻¹) ^d
1	Aeroxide P25	76	66	87	4 407
2	Commercial anatase	9	9	99	472
3	Anatase prepared <i>via</i> sol-gel method	21	17	81	1 101

^a Reaction conditions: benzylamine (0.24 mmol, 1 eq.), 3 mL MeCN, N₂O atmosphere (0.29 mmol in gas phase, 7 mL, 1.2 eq.), 10 mg Ag/TiO₂ (0.3 wt%), *i.e.* substrate/metal = 1 000, 365 nm irradiation (two LEDs, 150 mW/cm²), 15 min. ^b Determined by Gas Chromatography analyses using chlorobenzene as internal standard. ^c Selectivity in imine product = yield/conversion. ^d Turnover frequency, equal to the molar quantity of amine transformed over surface silver molar quantity over time unit.

Metal loading for cross-coupling reactions



a) 1 mol% metal loading (alcohol/metal = 100)



b) 0.1 mol% metal loading (alcohol/metal = 1000)

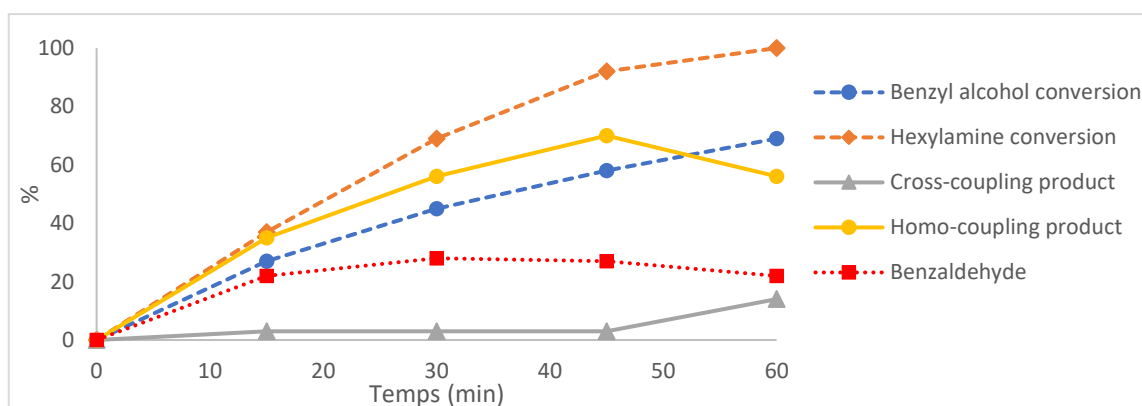
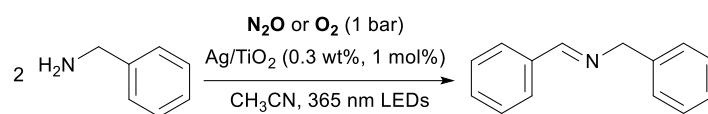


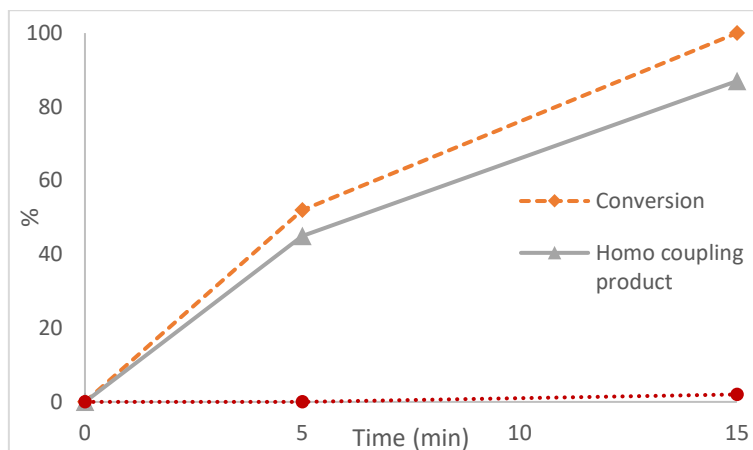
Figure S7: Kinetics for the influence of the metal loading (a: 1 mol%, b: 0.1 mol%) on the cross-coupling of benzyl alcohol and hexylamine under N_2O atmosphere.

^a Reaction conditions: benzyl alcohol (0.24 mmol, 1 eq.), hexylamine (0.24 mmol, 1 eq.), 3 mL MeCN, N_2O atmosphere (0.29 mmol in gas phase, 7 mL, 1.2 eq.), catalyst Ag/TiO_2 (0.3 wt%, TiO_2 Aeroxide P25), 100 mg: 1 mol% *i.e.* alcohol/metal = 100, or 10 mg: 0.1 mol% *i.e.* alcohol/metal = 1 000, 365 nm irradiation (two LEDs, 150 mW/cm^2). Conversions and yields determined by Gas Chromatography analyses using chlorobenzene as internal standard. Relative yield based on the peak area for the cross-coupling product. The homo-coupling product was defined as the N-Hexyl-1-hexanimine.

Selectivity: N₂O vs. O₂



a) N₂O atmosphere



b) O₂ atmosphere

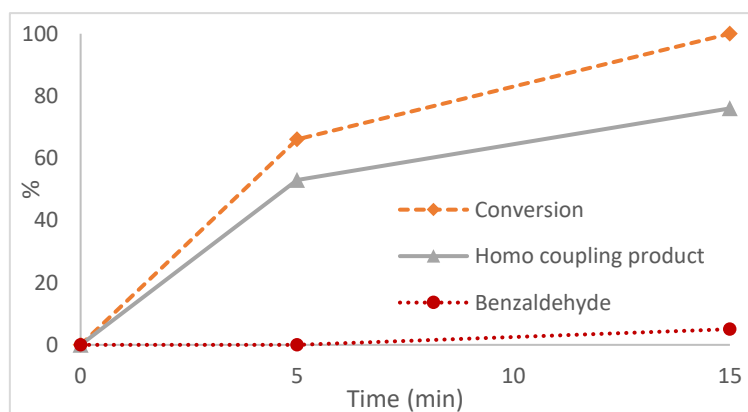
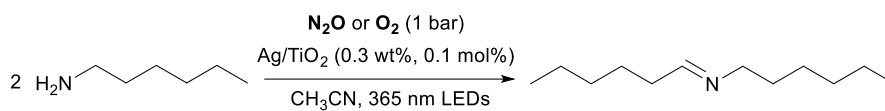
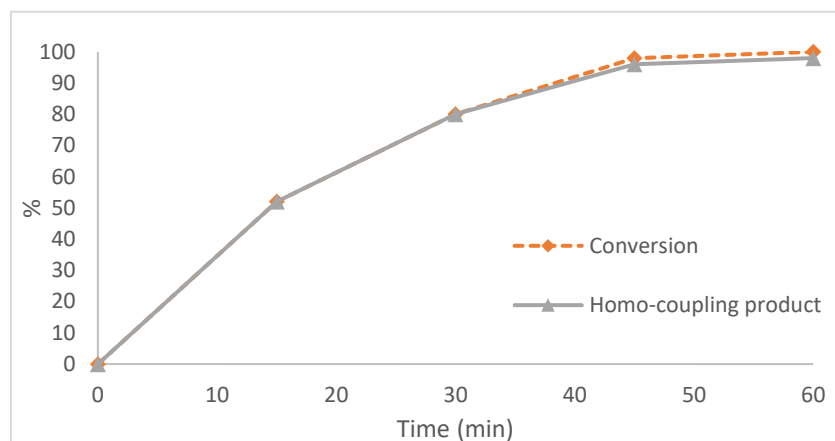


Figure S8: Kinetics for homo-coupling of benzylamine under N₂O atmosphere (a), and O₂ atmosphere (b).

^a Reaction conditions: benzylamine (0.24 mmol, 1 eq.), 3 mL MeCN, N₂O or O₂ atmosphere (7 mL gas phase), 100 mg Ag/TiO₂ (0.3 wt%, TiO₂ Aeroxide P25), *i.e.* amine/metal = 100, 365 nm irradiation (two LEDs, 150 mW/cm²), 15 min. Conversions and yields determined by Gas Chromatography analyses using chlorobenzene as internal standard.



a) N₂O atmosphere



b) O₂ atmosphere

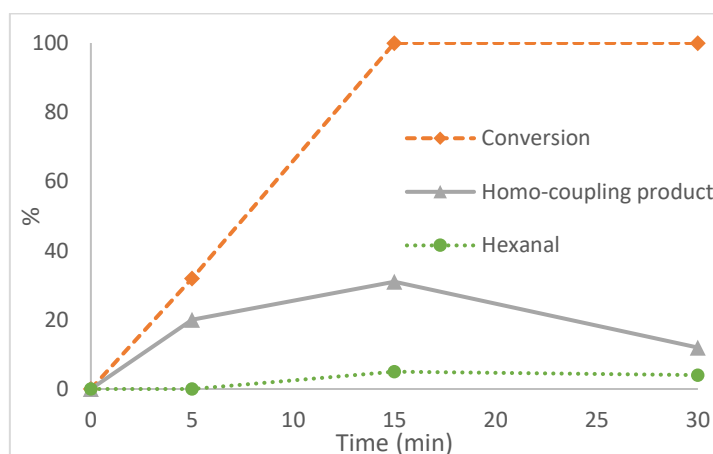
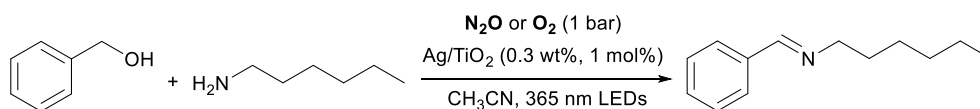
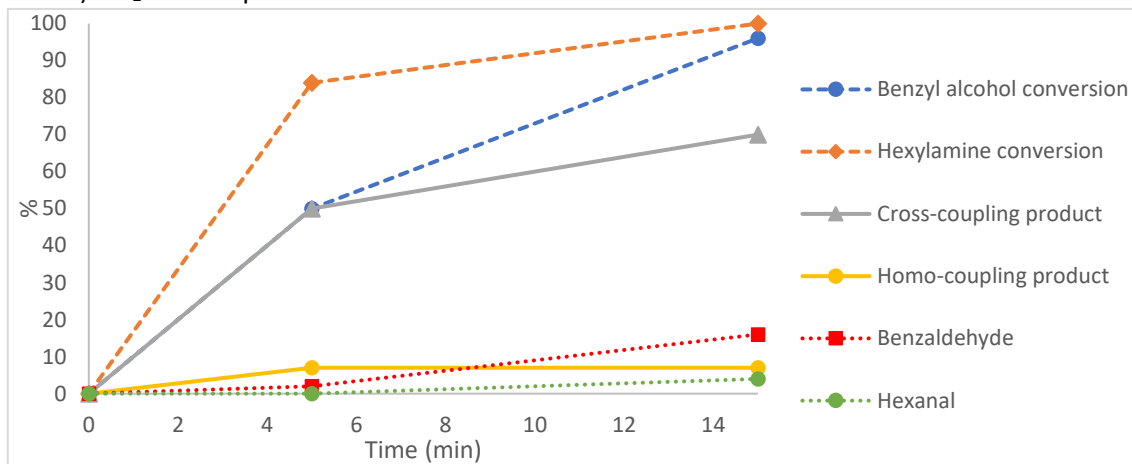


Figure S9: Kinetics for homo-coupling of hexylamine under N₂O atmosphere (a), and O₂ atmosphere (b).

^a Reaction conditions: hexylamine (0.24 mmol, 1 eq.), 3 mL MeCN, N₂O or O₂ atmosphere (7 mL gas phase), 100 mg Ag/TiO₂ (0.3 wt%, TiO₂ Aeroxide P25), *i.e.* amine/metal = 100, 365 nm irradiation (two LEDs, 150 mW/cm²), 15 min. Conversions and yields determined by Gas Chromatography analyses using chlorobenzene as internal standard.



a) N₂O atmosphere



b) O₂ atmosphere

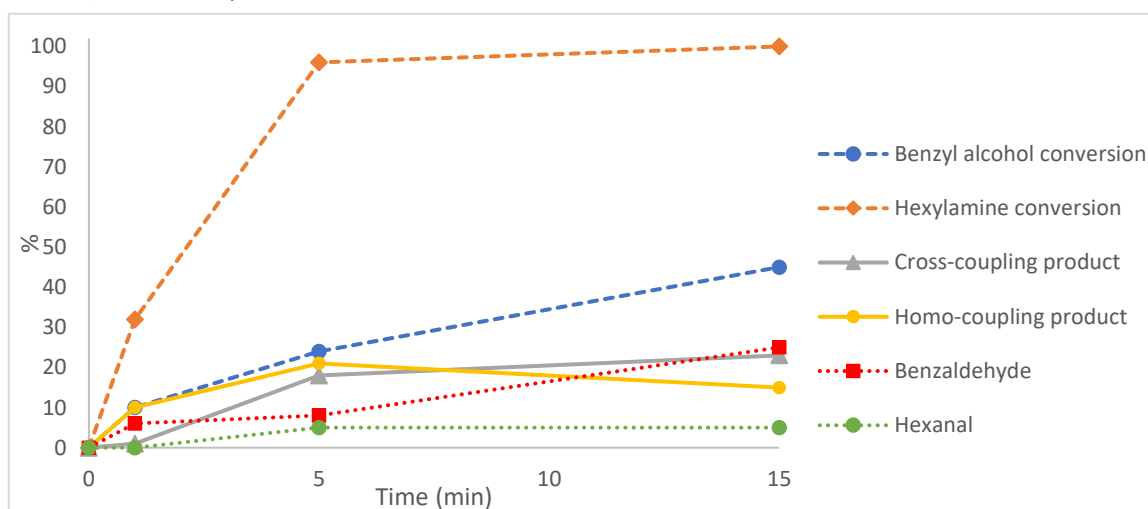


Figure S10: Kinetics for cross-coupling of benzyl alcohol and hexylamine under N₂O atmosphere (a), and O₂ atmosphere (b).

^a Reaction conditions: benzyl alcohol (0.24 mmol, 1 eq.), hexylamine (0.24 mmol, 1 eq.), 3 mL MeCN, N₂O or O₂ atmosphere (7 mL gas phase), 100 mg Ag/TiO₂ (0.3 wt%, TiO₂ Aeroxide P25), *i.e.* alcohol/metal = 100, 365 nm irradiation (two LEDs, 150 mW/cm²), 15 min. Conversions and yields determined by Gas Chromatography analyses using chlorobenzene as internal standard. Relative yield based on the peak area for the cross-coupling product. The homo-coupling product was defined as the N-Hexyl-1-hexanimine.

Benzylamine homo-coupling with molecular sieve

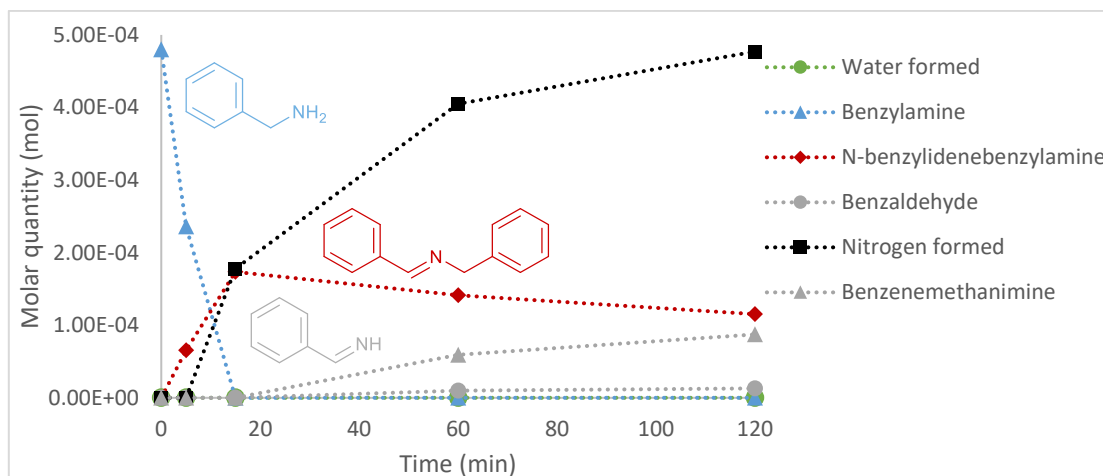
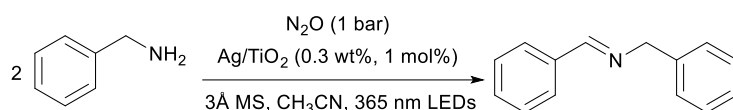


Figure S11: Kinetics of benzylamine homo-coupling under anhydrous conditions in the presence of molecular sieve.

Reaction conditions: benzylamine (0.48 mmol, 1 eq.), 6 mL MeCN, N₂O atmosphere (0.78 mmol in gas phase, 19 mL, 1.6 eq.), 200 mg Ag/TiO₂ (0.3 wt%), *i.e.* amine/silver = 100, 365 nm irradiation (two LEDs, 150 mW/cm²), 300 mg of 3Å activated molecular sieves. Benzylamine (blue triangles), *N*-benzyl-1-phenylmethanimine (red diamonds), benzaldehyde (grey circles), and phenylmethanimine (grey triangles) quantities determined by Gas Chromatography analyses using chlorobenzene as internal standard. N₂ (black squares) quantified by GC-BID detector. H₂O content (green circles) quantified with a Karl Fischer titrator.

Recycling tests

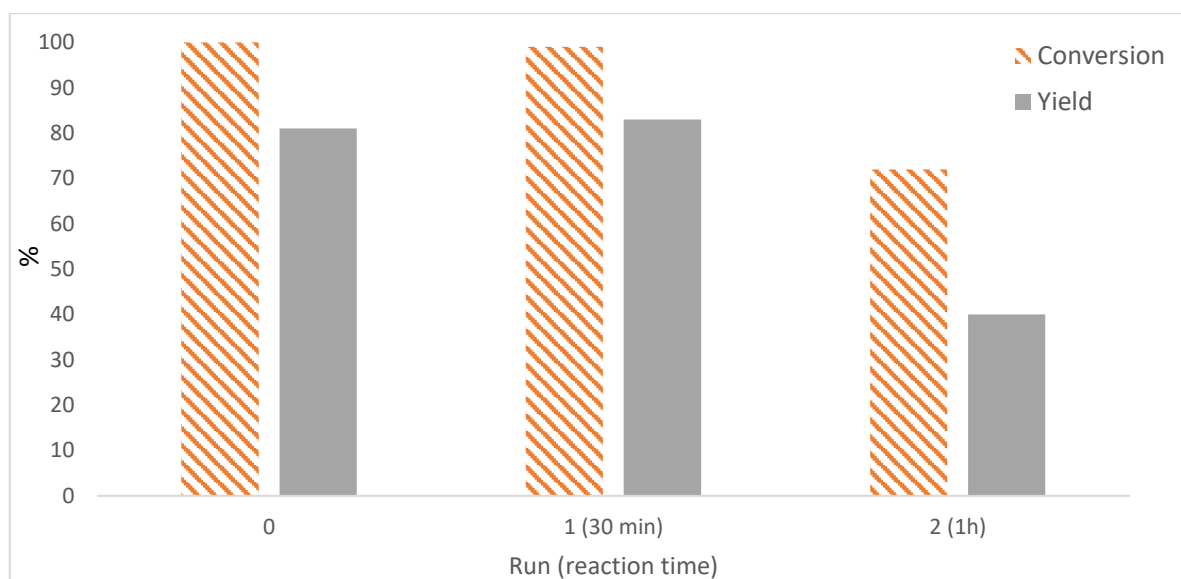


Figure S12: Recycling tests of the catalyst in the photo-oxidative coupling of benzylamine.

Reaction conditions: benzylamine (0.96 mmol for run 0), solvent MeCN (12 mL for run 0), N₂O atmosphere, catalyst Ag/TiO₂ (0.3 wt%, TiO₂ Aeroxide P25), 1 mol% *i.e.* amine/metal = 100 (400 mg for run 0), 365 nm irradiation (two LEDs, 150 mW/cm²), 15 min for run 0. Isolated yield for run 0. Conversion and yield determined by Gas Chromatography analyses using chlorobenzene as internal standard for runs 1 and 2.

After photo-oxidative homo-coupling of benzylamine, the catalyst (which turned brownish during the reaction) was isolated by centrifugation (5 min; 4 000 rpm), washed 3 times with acetonitrile and dried at least one night in an oven at 80 °C. The recycled catalyst was then grinded manually to recover fine particles, activated under oxygen flow for 4h at 130 °C, and weighed. Between 10 and 20 % of the mass of the catalyst was lost after each recycling, therefore quantities of benzylamine and solvent were adapted to keep the same conditions (1 mol%; 80 mmol/L).

For each run, the quantity of N₂ formed during the reaction was measured and was equivalent to the conversion rate of the starting amine.

NMR data

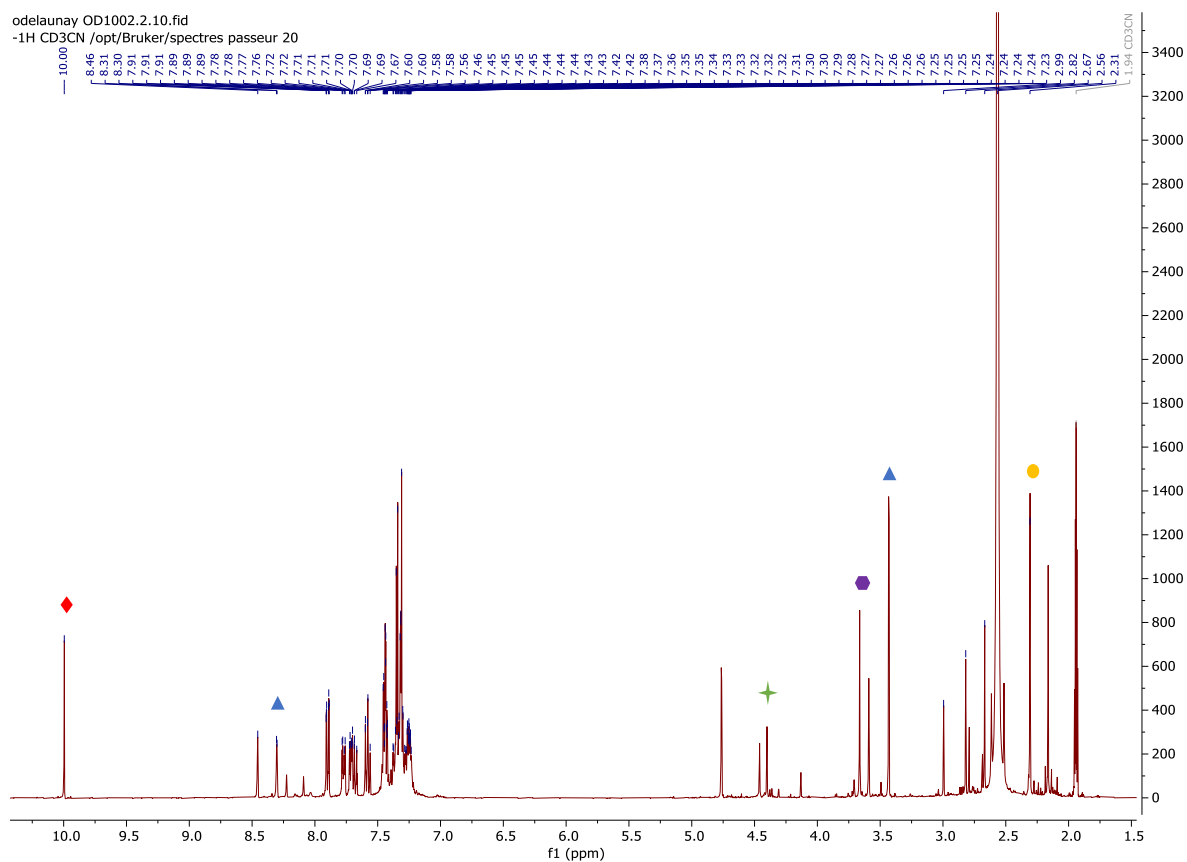


Figure S13: ^1H NMR spectra after photo-oxidation of N-methylbenzylamine under standard conditions to check methylamine formation (unpurified mixture), with signal of methylamine at 2.31 ppm (●), and characteristic signals of N-methyl-1-phenylmethanimine (▲), benzaldehyde (◆), and N,N'-dimethyl-1-phenylmethanediamine (✚) formed, and remaining starting material (●) (400 MHz, CD_3CN).

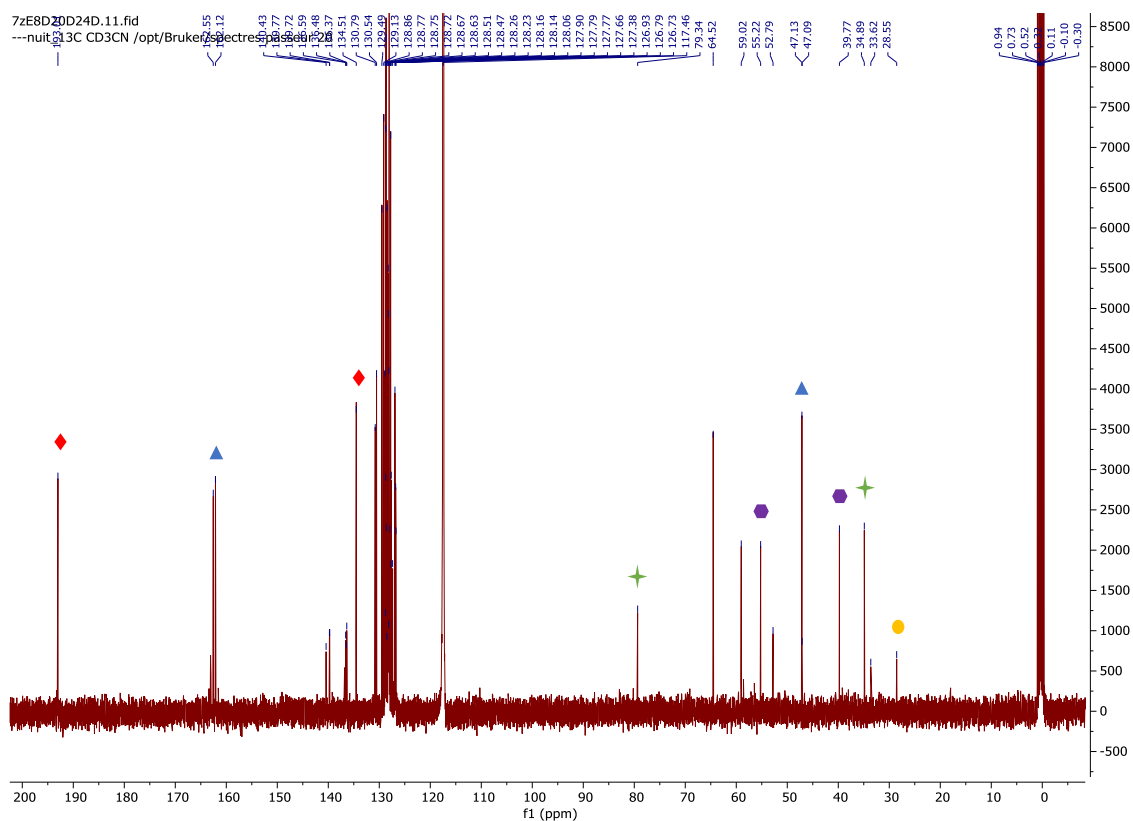


Figure S14: ^{13}C NMR spectra after photo-oxidation of N-methylbenzylamine under standard conditions to check methylamine formation (unpurified mixture), with signal of methylamine at 28.55 ppm (●), and characteristic signals of N-methyl-1-phenylmethanimine (▲), benzaldehyde (◆), and N,N'-dimethyl-1-phenylmethanediamine (⊕) formed, and remaining starting material (●) (100 MHz, CD_3CN).

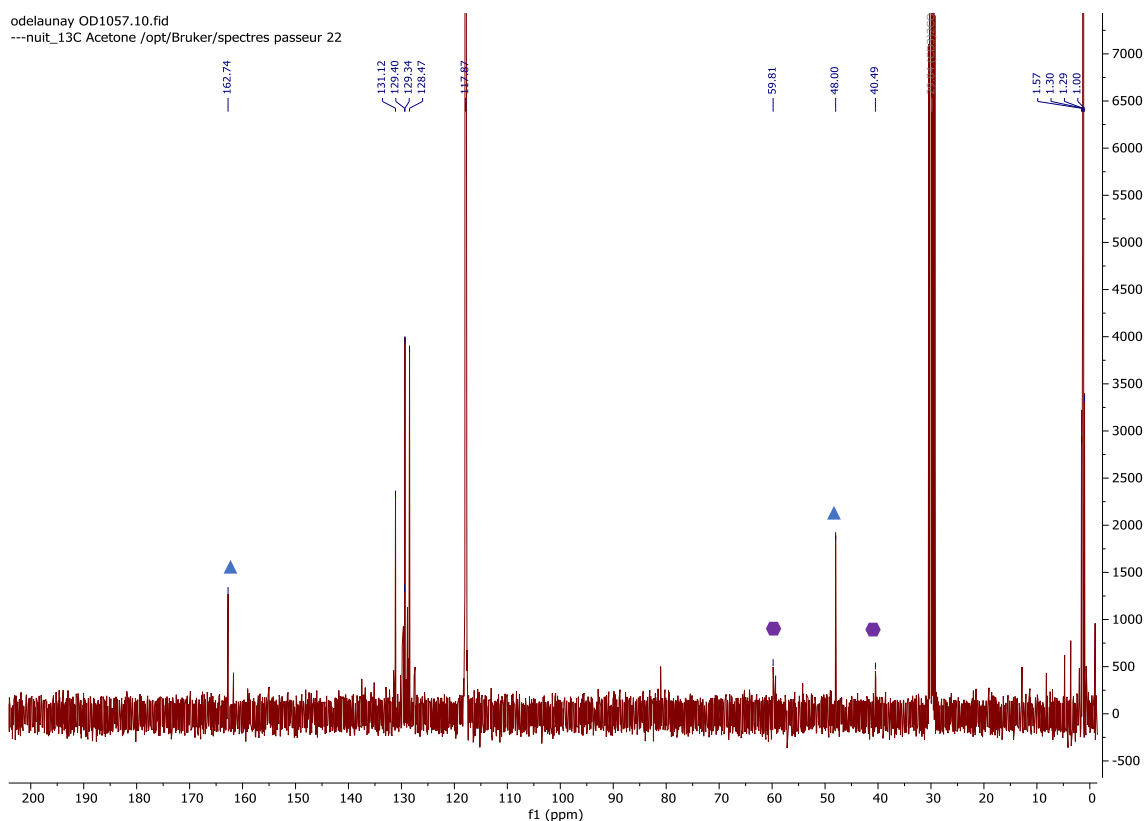
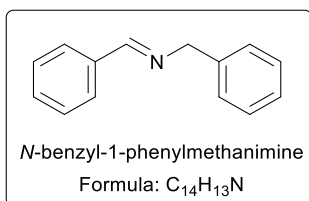


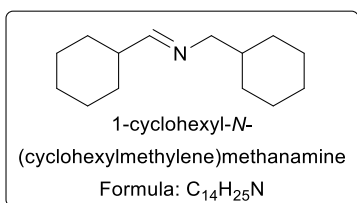
Figure S15: ^{13}C NMR spectra after photo-oxidation of N-methylbenzylamine with activated molecular sieves to check methylamine formation (unpurified mixture), with characteristic signals of N-methyl-1-phenylmethanimine (\blacktriangle) formed, and remaining starting material (\bullet) (100 MHz, $(\text{CD}_3)_2\text{CO}$).



83 % isolated yield, yellowish oil.

^1H NMR (400 MHz, CDCl_3): δ 8.38 (1 H, s, CH), 7.80-7.77 (2 H, m, ar, $J=4.0$ Hz), 7.41-7.21 (8 H, m, ar, $J=4$ Hz), 4.82 (2 H, s, CH_2).

^{13}C NMR (100 MHz, CDCl_3): δ 162.06; 139.41; 136.27; 130.85; 128.69; 128.59; 128.37; 128.07; 127.08; 65.14.



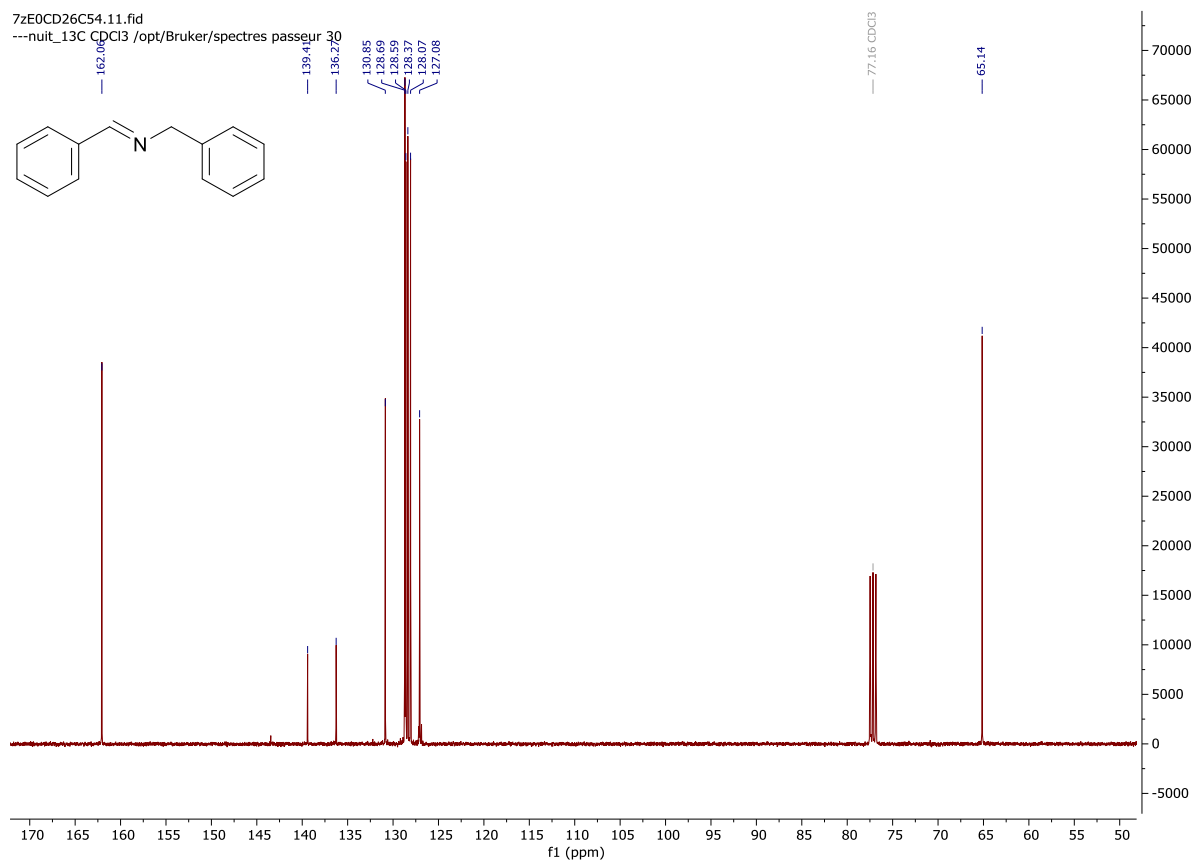
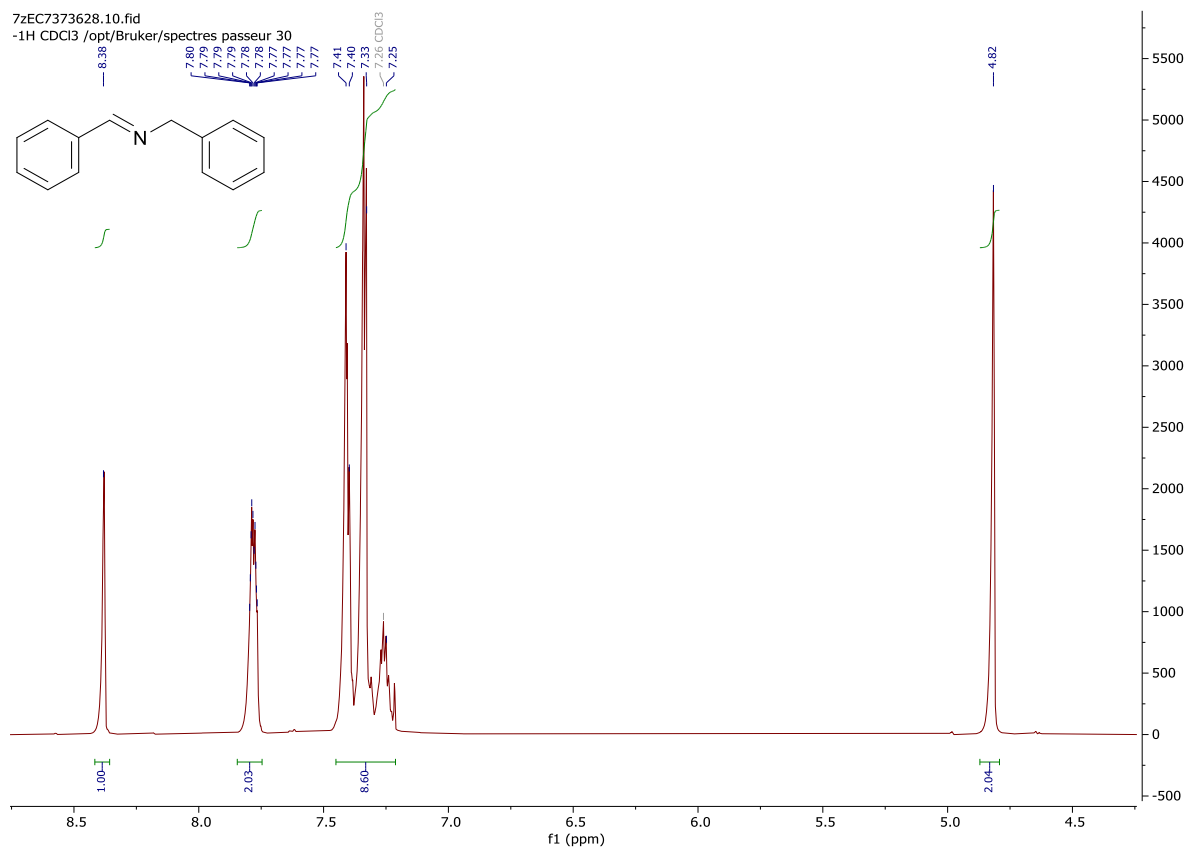
67 % isolated yield, yellowish oil.

^1H NMR (400 MHz, C_6D_6): δ 7.35 (1 H, s, CH), 3.20 (2 H, d, CH_2), 2.12-2.05 (1 H, m, CH), 1.81-1.76 (4 H, m, CH_2), 1.72-1.60 (6 H, m, CH_2), 1.29-1.11 (9 H, m, $\text{CH}_2\text{-CH}$), 1.00-0.91 (2 H, m, CH_2).

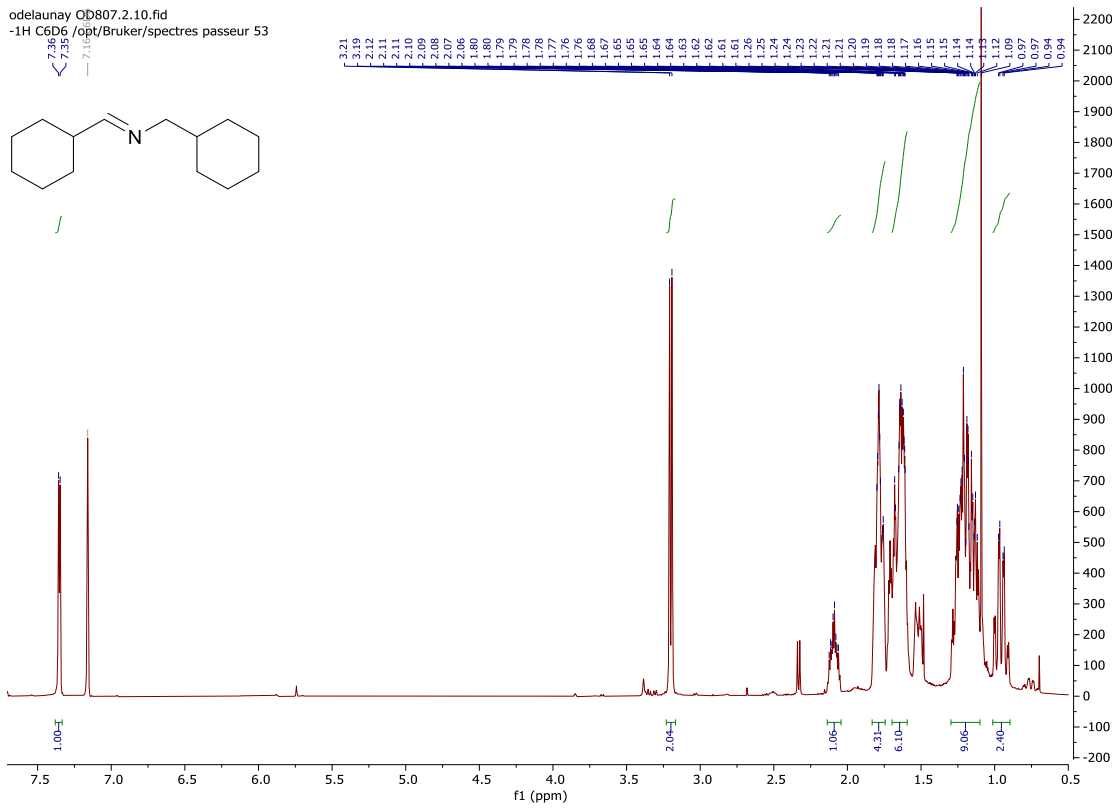
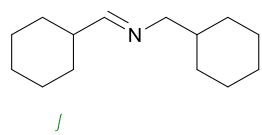
^{13}C NMR (100 MHz, C_6D_6): δ 167.63; 69.07; 43.69; 39.54; 32.01;

30.37; 27.34; 26.82-26.80; 26.17; 13.80.

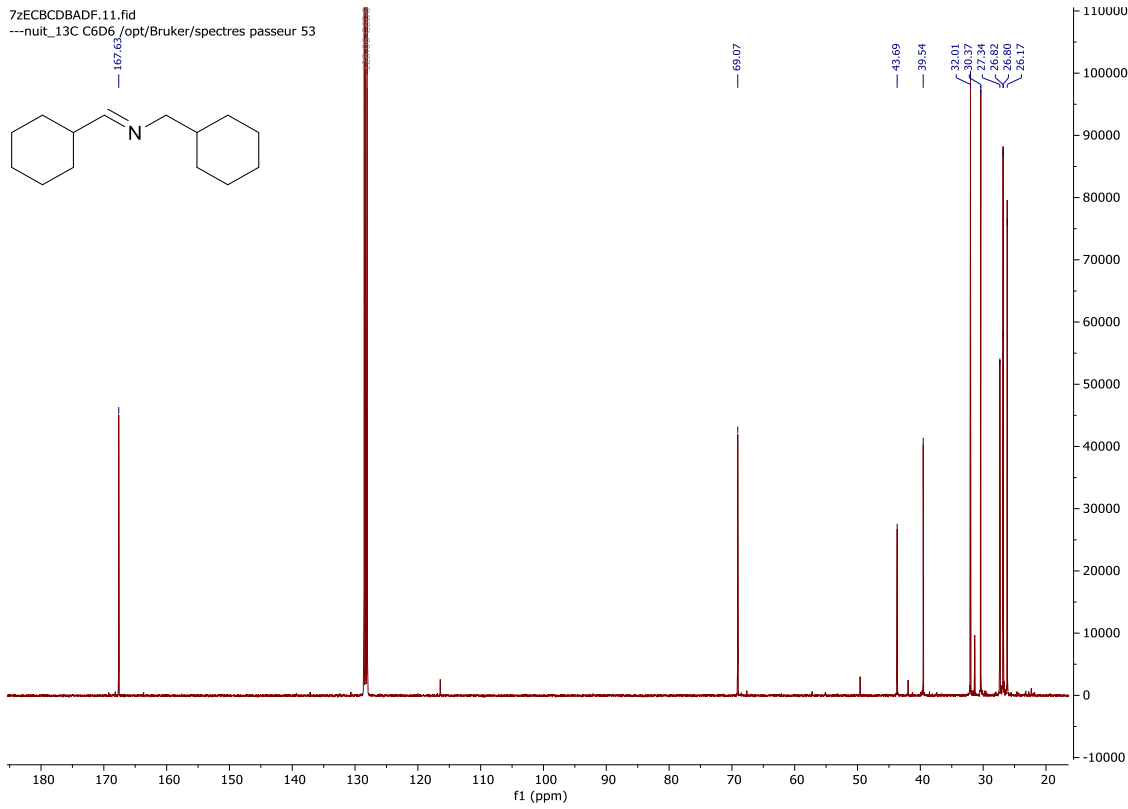
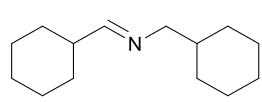
NMR spectra



odelaunay QD807.2.10.fid
 -1H C6D6 /opt/Bruker/spectres passeur 53



7zECBCBADF.11.fid
 ---nuit_13C C6D6 /opt/Bruker/spectres passeur 53



References

- 1 E. Albiter, M. A. Valenzuela, S. Alfaro, G. Valverde-Aguilar and F. M. Martínez-Pallares, *Journal of Saudi Chemical Society*, 2015, **19**, 563–573.
- 2 O. Delaunay, E. Zghab, A. Denicourt-Nowicki and A. Roucoux, *ChemCatChem*, 2023, **15**, e202201517.
- 3 A. P. Umpierre, E. de Jesús and J. Dupont, *ChemCatChem*, 2011, **3**, 1413–1418.